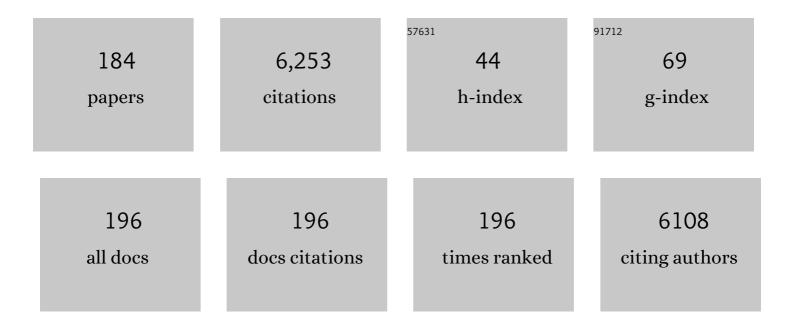
List of Publications by Year in descending order

Source: https://exaly.com/author-pdf/4860415/publications.pdf Version: 2024-02-01



#	Article	IF	CITATIONS
1	Solution structure of a specific DNA complex of the Myb DNA-binding domain with cooperative recognition helices. Cell, 1994, 79, 639-648.	13.5	486
2	The cavity in the hydrophobic core of Myb DNA-binding domain is reserved for DNA recognition and trans-activation. Nature Structural Biology, 1996, 3, 178-187.	9.7	243
3	Most compact hairpin-turn structure exerted by a short DNA fragment, d(GCGAAGC) in solution: an extraordinarily stable structure resistant to nucleases and heat. Nucleic Acids Research, 1994, 22, 576-582.	6.5	203
4	Comparison of the free and DNA-complexed forms of the DMA-binding domain from c-Myb. Nature Structural and Molecular Biology, 1995, 2, 309-320.	3.6	156
5	Extraordinarily stable mini-hairpins: electrophoretical and thermal properties of the various sequence variants of d(GCFAAAGC)and their effect on DNA sequencing. Nucleic Acids Research, 1992, 20, 3891-3896.	6.5	140
6	Confined water-mediated high proton conduction in hydrophobic channel of a synthetic nanotube. Nature Communications, 2020, 11, 843.	5.8	116
7	Comparison between TRF2 and TRF1 of their telomeric DNA-bound structures and DNA-binding activities. Protein Science, 2009, 14, 119-130.	3.1	109
8	In-plane vibrational modes in the uracil molecule from an ab initio MO calculation. Journal of the American Chemical Society, 1981, 103, 1354-1358.	6.6	106
9	Conformation-sensitive Raman lines of mononucleotides and their use in a structure analysis of polynucleotides: guanine and cytosine nucleotides. Journal of Molecular Structure, 1986, 146, 123-153.	1.8	104
10	A Free-Energy Landscape for Coupled Folding and Binding of an Intrinsically Disordered Protein in Explicit Solvent from Detailed All-Atom Computations. Journal of the American Chemical Society, 2011, 133, 10448-10458.	6.6	102
11	Structural comparison of the PhoB and OmpR DNA-binding/transactivation domains and the arrangement of PhoB molecules on the phosphate box. Journal of Molecular Biology, 2000, 295, 1225-1236.	2.0	90
12	Growth of carbon nanotubes via twisted graphene nanoribbons. Nature Communications, 2013, 4, 2548.	5.8	89
13	Three pillars for achieving quantum mechanical molecular dynamics simulations of huge systems: Divideâ€andâ€conquer, densityâ€functional tightâ€binding, and massively parallel computation. Journal of Computational Chemistry, 2016, 37, 1983-1992.	1.5	88
14	Escherichia coli positive regulator OmpR has a large loop structure at the putative RNA polymerase interaction site. Nature Structural and Molecular Biology, 1997, 4, 28-31.	3.6	87
15	Dimerization-Initiated Preferential Formation of Coronene-Based Graphene Nanoribbons in Carbon Nanotubes. Journal of Physical Chemistry C, 2012, 116, 15141-15145.	1.5	87
16	Extraordinary stable structure of short single-stranded DNA fragments containing a specific base sequence: d(GCGAAAGC). Nucleic Acids Research, 1989, 17, 2223-2231.	6.5	86
17	Common TFIIH recruitment mechanism in global genome and transcription-coupled repair subpathways. Nucleic Acids Research, 2017, 45, 13043-13055.	6.5	83
18	Sodium―and Potassiumâ€Hydrate Melts Containing Asymmetric Imide Anions for Highâ€Voltage Aqueous Batteries. Angewandte Chemie - International Edition, 2019, 58, 14202-14207.	7.2	81

#	Article	IF	CITATIONS
19	Collective vibrational modes in molecular assembly of DNA and its application to biological systems. Low frequency Raman spectroscopy. Journal of Chemical Physics, 1985, 82, 531-535.	1.2	80
20	A Protein Kinase Cδ-binding Protein SRBC Whose Expression Is Induced by Serum Starvation. Journal of Biological Chemistry, 1997, 272, 7381-7389.	1.6	77
21	Solution Structure of a Telomeric DNA Complex of Human TRF1. Structure, 2001, 9, 1237-1251.	1.6	77
22	Crystal structure of the overlapping dinucleosome composed of hexasome and octasome. Science, 2017, 356, 205-208.	6.0	77
23	The Neural Repressor NRSF/REST Binds the PAH1 Domain of the Sin3 Corepressor by Using its Distinct Short Hydrophobic Helix. Journal of Molecular Biology, 2005, 354, 903-915.	2.0	76
24	Infrared identification of the Criegee intermediates syn- and anti-CH3CHOO, and their distinct conformation-dependent reactivity. Nature Communications, 2015, 6, 7012.	5.8	74
25	Coupled dynamics between DNA double helix and hydrated water by low frequency Raman spectroscopy. Journal of Chemical Physics, 1985, 83, 5972-5975.	1.2	70
26	Function of homo- and hetero-oligomers of human nucleoplasmin/nucleophosmin family proteins NPM1, NPM2 and NPM3 during sperm chromatin remodeling. Nucleic Acids Research, 2012, 40, 4861-4878.	6.5	67
27	Characterization of a few Raman lines of tryptophan. Journal of Raman Spectroscopy, 1978, 7, 282-287.	1.2	63
28	N-terminal phosphorylation of HP1α increases its nucleosome-binding specificity. Nucleic Acids Research, 2014, 42, 12498-12511.	6.5	63
29	Impact of nucleic acid and methylated H3K9 binding activities of Suv39h1 on its heterochromatin assembly. ELife, 2017, 6, .	2.8	61
30	D <scp>cdftbmd</scp> : Divideâ€andâ€Conquer Density Functional Tightâ€Binding Program for Hugeâ€System Quantum Mechanical Molecular Dynamics Simulations. Journal of Computational Chemistry, 2019, 40, 1538-1549.	1.5	58
31	Solution structure of the DNA-binding domain of human telomeric protein, hTRF1. Structure, 1998, 6, 1057-1065.	1.6	56
32	NMR structure of the hrap1 myb motif reveals a canonical three-helix bundle lacking the positive surface charge typical of myb DNA-binding domains 1 1Edited by P. E. Wright. Journal of Molecular Biology, 2001, 312, 167-175.	2.0	55
33	Automatized Parameterization of DFTB Using Particle Swarm Optimization. Journal of Chemical Theory and Computation, 2016, 12, 53-64.	2.3	55
34	Solution structure of the transactivation domain of ATF-2 comprising a zinc finger-like subdomain and a flexiblesubdomain. Journal of Molecular Biology, 1999, 287, 593-607.	2.0	54
35	Intrinsic Nucleic Acid-Binding Activity of Chp1 Chromodomain Is Required for Heterochromatic Gene Silencing. Molecular Cell, 2012, 47, 228-241.	4.5	53
36	Divide-and-Conquer-Type Density-Functional Tight-Binding Molecular Dynamics Simulations of Proton Diffusion in a Bulk Water System. Journal of Physical Chemistry B, 2016, 120, 217-221.	1.2	53

#	Article	IF	CITATIONS
37	Structure-spectrum correlations in nucleic acids. I. Raman lines in the 600–700 cmâ~'1range of guanosine residue. Nucleic Acids Research, 1984, 12, 6901-6908.	6.5	52
38	Structural insight into the TFIIE–TFIIH interaction: TFIIE and p53 share the binding region on TFIIH. EMBO Journal, 2008, 27, 1161-1171.	3.5	51
39	Location of phosphorylation site and DNA-binding site of a positive regulator, OmpR, involved in activation of the osmoregulatory genes ofEscherichia coli. FEBS Letters, 1989, 249, 168-172.	1.3	50
40	Structural genomics projects in Japan. Progress in Biophysics and Molecular Biology, 2000, 73, 363-376.	1.4	49
41	Structural Basis of Homology-Directed DNA Repair Mediated by RAD52. IScience, 2018, 3, 50-62.	1.9	49
42	An A-form poly(dG) · poly(dC) in H2O solution. Biopolymers, 1985, 24, 1841-1844.	1.2	47
43	In-plane vibrational modes of cytosine from an ab initio MO calculation. Chemical Physics, 1985, 98, 71-80.	0.9	46
44	Local and overall conformations of DNA double helices with the A·T base pairs. Biochimica Et Biophysica Acta Gene Regulatory Mechanisms, 1986, 867, 256-267.	2.4	45
45	Location of DNA-binding segment of a positive regulator, OmpR, involved in activation of theompFandompCgenes ofEscherichia coli. FEBS Letters, 1988, 242, 27-30.	1.3	45
46	Extended String Binding Mode of the Phosphorylated Transactivation Domain of Tumor Suppressor p53. Journal of the American Chemical Society, 2014, 136, 14143-14152.	6.6	45
47	Infrared spectrum of trans-acrolein. Chemical Physics, 1985, 100, 365-375.	0.9	44
48	Proton nuclear magnetic resonance studies of the structure of the Fc fragment of human immunoglobulin G1: Comparisons of native and recombinant proteins. Molecular Immunology, 1990, 27, 571-579.	1.0	43
49	Internal motion of deoxyribonucleic acid in chromatin. Nanosecond fluorescence studies of intercalated ethidium. Biochemistry, 1983, 22, 6018-6026.	1.2	42
50	In-Plane Vibrational Modes of Guanine from an abInitioMO Calculation. Bulletin of the Chemical Society of Japan, 1985, 58, 638-645.	2.0	42
51	Novel Structural and Functional Mode of a Knot Essential for RNA Binding Activity of the Esa1 Presumed Chromodomain. Journal of Molecular Biology, 2008, 378, 987-1001.	2.0	42
52	Structural visualization of key steps in nucleosome reorganization by human FACT. Scientific Reports, 2019, 9, 10183.	1.6	42
53	Raman spectra of flavins: avoidance of interference from fluorescence. Chemical Physics Letters, 1978, 59, 210-213.	1.2	41
54	A Mass Spectrometric Approach to the Study of DNA-Binding Proteins:  Interaction of Human TRF2 with Telomeric DNA. Biochemistry, 2008, 47, 1797-1807.	1.2	39

#	Article	IF	CITATIONS
55	Divide-and-Conquer-Type Density-Functional Tight-Binding Simulations of Hydroxide Ion Diffusion in Bulk Water. Journal of Physical Chemistry B, 2017, 121, 1362-1371.	1.2	38
56	Rigorous p <i>K</i> _a Estimation of Amine Species Using Density-Functional Tight-Binding-Based Metadynamics Simulations. Journal of Chemical Theory and Computation, 2018, 14, 351-356.	2.3	38
57	On the excited-state geometry of the adenine residue as revealed by a preresonance Raman effect. Journal of Raman Spectroscopy, 1974, 2, 609-621.	1.2	37
58	Ultraviolet resonance Raman bands of guanosine and adenosine residues useful for the determination of nucleic acid conformation. Journal of Raman Spectroscopy, 1987, 18, 221-227.	1.2	36
59	Top-down analysis of basic proteins by microchip capillary electrophoresis mass spectrometry. Rapid Communications in Mass Spectrometry, 2006, 20, 1932-1938.	0.7	36
60	Dramatic Reduction of IR Vibrational Cross Sections of Molecules Encapsulated in Carbon Nanotubes. Journal of the American Chemical Society, 2011, 133, 8191-8198.	6.6	36
61	Application of 13C Nuclear Magnetic Resonance Spectroscopy to Molecular Structural Analyses of Antibody Molecules1. Journal of Biochemistry, 1989, 105, 867-869.	0.9	34
62	Contrasting mechanisms for CO2 absorption and regeneration processes in aqueous amine solutions: Insights from density-functional tight-binding molecular dynamics simulations. Chemical Physics Letters, 2016, 647, 127-131.	1.2	34
63	On the base-stacking in the 5′-terminal cap structure of mRNA: a fluorescence study. Nucleic Acids Research, 1980, 8, 1107-1119.	6.5	33
64	A Novel Zinc Finger Structure in the Large Subunit of Human General Transcription Factor TFIIE. Journal of Biological Chemistry, 2004, 279, 51395-51403.	1.6	32
65	Divide-and-Conquer Density-Functional Tight-Binding Molecular Dynamics Study on the Formation of Carbamate Ions during CO2 Chemical Absorption in Aqueous Amine Solution. Bulletin of the Chemical Society of Japan, 2017, 90, 1230-1235.	2.0	32
66	Waterâ€mediated interactions between DNA and PhoB DNAâ€binding/transactivation domain: NMRâ€restrained molecular dynamics in explicit water environment. Proteins: Structure, Function and Bioinformatics, 2008, 71, 1970-1983.	1.5	31
67	Acetylated histone H4 tail enhances histone H3 tail acetylation by altering their mutual dynamics in the nucleosome. Proceedings of the National Academy of Sciences of the United States of America, 2020, 117, 19661-19663.	3.3	31
68	Interaction of Acetone with Single Wall Carbon Nanotubes at Cryogenic Temperatures: A Combined Temperature Programmed Desorption and Theoretical Study. Langmuir, 2008, 24, 7848-7856.	1.6	30
69	Structural Insight into the Mechanism of TFIIH Recognition by the Acidic String of the Nucleotide Excision Repair Factor XPC. Structure, 2015, 23, 1827-1837.	1.6	30
70	Parallel implementation of efficient charge–charge interaction evaluation scheme in periodic divideâ€andâ€conquer densityâ€functional tightâ€binding calculations. Journal of Computational Chemistry, 2018, 39, 105-116.	1.5	29
71	Structural Polymorphism of Chromodomains in Chd1. Journal of Molecular Biology, 2007, 365, 1047-1062.	2.0	28
72	Solution structure of the isolated histone H2A-H2B heterodimer. Scientific Reports, 2016, 6, 24999.	1.6	28

#	Article	IF	CITATIONS
73	On the Normal Modes of Vibration in the Uracil Residue—The Use of15N-Isotope Effects. Bulletin of the Chemical Society of Japan, 1979, 52, 1340-1345.	2.0	26
74	Conclusive Evidence of the Reconstituted Hexasome Proven by Native Mass Spectrometry. Biochemistry, 2013, 52, 5155-5157.	1.2	26
75	Theoretical study of cellobiose hydrolysis to glucose in ionic liquids. Chemical Physics Letters, 2014, 603, 7-12.	1.2	26
76	Evaluation of protein-DNA binding affinity by electrospray ionization mass spectrometry. Journal of the American Society for Mass Spectrometry, 2005, 16, 116-125.	1.2	25
77	I-motif and quadruplex-based device that can control a protein release or bind and release small molecule to influence biological processes. Bioorganic and Medicinal Chemistry, 2007, 15, 1275-1279.	1.4	25
78	Selective dissociation of non-covalent bonds in biological molecules by laser spray. Journal of Mass Spectrometry, 2004, 39, 1053-1058.	0.7	24
79	GPUâ€Accelerated Largeâ€Scale Excitedâ€State Simulation Based on Divideâ€and onquer Timeâ€Dependent Densityâ€Functional Tightâ€Binding. Journal of Computational Chemistry, 2019, 40, 2778-2786.	1.5	24
80	Extended string-like binding of the phosphorylated HP1α N-terminal tail to the lysine 9-methylated histone H3 tail. Scientific Reports, 2016, 6, 22527.	1.6	23
81	Lifetime of Tyrosine Fluorescence in Nucleosome Core Particles1. Journal of Biochemistry, 1982, 91, 2047-2055.	0.9	22
82	Spectrophotometric and resonance Raman studies on the formation of phenolate and thiolate complexes of (octaethylporphinato)iron(III). Inorganic Chemistry, 1990, 29, 2803-2807.	1.9	22
83	Gas-Phase Structure of the Histone Multimers Characterized by Ion Mobility Mass Spectrometry and Molecular Dynamics Simulation. Analytical Chemistry, 2013, 85, 4165-4171.	3.2	22
84	Large-Scale Molecular Dynamics Simulation for Ground and Excited States Based on Divide-and-Conquer Long-Range Corrected Density-Functional Tight-Binding Method. Journal of Chemical Theory and Computation, 2020, 16, 2369-2378.	2.3	22
85	Increased stability of the higher order structure of chicken erythrocyte chromatin: nanosecond anisotropy studies of intercalated ethidium. Biochemistry, 1985, 24, 1291-1297.	1.2	21
86	Câ€ŧerminal acidic domain of histone chaperone human <scp>NAP</scp> 1 is an efficient binding assistant for histone H2Aâ€H2B, but not H3â€H4. Genes To Cells, 2016, 21, 252-263.	0.5	21
87	A mimetic of the mSin3-binding helix of NRSF/REST ameliorates abnormal pain behavior in chronic pain models. Bioorganic and Medicinal Chemistry Letters, 2017, 27, 4705-4709.	1.0	21
88	Investigation of the Pyrimidine Preference by the c-Myb DNA-binding Domain at the Initial Base of the Consensus Sequence. Journal of Biological Chemistry, 1997, 272, 17966-17971.	1.6	20
89	Deimination stabilizes histone H2A/H2B dimers as revealed by electrospray ionization mass spectrometry. Journal of Mass Spectrometry, 2010, 45, 900-908.	0.7	20
90	Telomeric repeats act as nucleosome-disfavouring sequences in vivo. Nucleic Acids Research, 2014, 42, 1541-1552.	6.5	20

#	Article	IF	CITATIONS
91	Substitutions of Conserved Aromatic Amino Acid Residues in Subunit I Perturb the Metal Centers of the Escherichia coli bo-Type Ubiquinol Oxidaseâ€. Biochemistry, 1998, 37, 1632-1639.	1.2	19
92	Temperature and pressure dependence of molecular adsorption on single wall carbon nanotubes and the existence of an "adsorption/desorption pressure gap― Carbon, 2010, 48, 1867-1875.	5.4	19
93	Time-resolved resonance Raman study of alkaline isomerization of ferricytochrome c. Biochemistry, 1984, 23, 6802-6808.	1.2	18
94	Stability analysis for double-stranded DNA oligomers and their noncovalent complexes with drugs by laser spray. Journal of Mass Spectrometry, 2006, 41, 1086-1095.	0.7	18
95	Sodium―and Potassiumâ€Hydrate Melts Containing Asymmetric Imide Anions for Highâ€Voltage Aqueous Batteries. Angewandte Chemie, 2019, 131, 14340-14345.	1.6	18
96	Raman spectra of transfer RNAs with ultraviolet lasers. Nature, 1976, 260, 173-174.	13.7	17
97	The structure of nucleosome core particles as revealed by difference Raman spectroscopy. Nucleic Acids Research, 1986, 14, 2583-2596.	6.5	17
98	Quantitative treatment of photochemical effects on ultraviolet resonance Raman spectroscopic intensities - application to enzymic cofactors containing dihydronicotinamide and their photochemically induced transients. Journal of the American Chemical Society, 1987, 109, 3514-3520.	6.6	17
99	Critical interpretation of CH– and OH– stretching regions for infrared spectra of methanol clusters (CH3OH) <i>n</i> (<i>n</i> = 2–5) using self-consistent-charge density functional tight-binding molecular dynamics simulations. Journal of Chemical Physics, 2014, 141, 094303.	1.2	17
100	Density-Functional Tight-Binding Molecular Dynamics Simulations of Excess Proton Diffusion in Ice I _h , Ice I _c , Ice III, and Melted Ice VI Phases. Journal of Physical Chemistry A, 2018, 122, 33-40.	1.1	17
101	Development of Large-Scale Excited-State Calculations Based on the Divide-and-Conquer Time-Dependent Density Functional Tight-Binding Method. Journal of Chemical Theory and Computation, 2019, 15, 1719-1727.	2.3	17
102	Evaluation of binding affinity of protein-mutant dna complexes in solution by laser spray mass spectrometry. Journal of the American Society for Mass Spectrometry, 2006, 17, 611-620.	1.2	16
103	Mechanism of Back Electron Transfer in an Intermolecular Photoinduced Electron Transfer Reaction: Solvent as a Charge Mediator. ChemPhysChem, 2014, 15, 2945-2950.	1.0	16
104	Sertraline, chlorprothixene, and chlorpromazine characteristically interact with the REST-binding site of the corepressor mSin3, showing medulloblastoma cell growth inhibitory activities. Scientific Reports, 2018, 8, 13763.	1.6	16
105	Hydroxide Ion Carrier for Proton Pumps in Bacteriorhodopsin: Primary Proton Transfer. Journal of Physical Chemistry B, 2020, 124, 8524-8539.	1.2	16
106	The N-terminal Tails of Histones H2A and H2B Adopt Two Distinct Conformations in the Nucleosome with Contact and Reduced Contact to DNA. Journal of Molecular Biology, 2021, 433, 167110.	2.0	16
107	Spectral Difference of the A and B Forms of Deoxyribonucleic Acid. Bulletin of the Chemical Society of Japan, 1974, 47, 1043-1044.	2.0	15
108	Epimerization and hydrolysis of etoposide analogues in aqueous solution Chemical and Pharmaceutical Bulletin, 1989, 37, 422-424.	0.6	15

#	Article	IF	CITATIONS
109	Structural Diversity of Nucleosomes Characterized by Native Mass Spectrometry. Analytical Chemistry, 2018, 90, 8217-8226.	3.2	15
110	Development of Divideâ€andâ€Conquer Densityâ€Functional Tightâ€Binding Method for Theoretical Research on Liâ€Ion Battery. Chemical Record, 2019, 19, 746-757.	2.9	15
111	Partial Replacement of Nucleosomal DNA with Human FACT Induces Dynamic Exposure and Acetylation of Histone H3 N-Terminal Tails. IScience, 2020, 23, 101641.	1.9	15
112	Self-complementary tetradeoxyribonucleoside triphosphates convenient chemical preparation and spectroscopic studies in solution. Tetrahedron, 1986, 42, 501-513.	1.0	14
113	Thermal unfolding of proteins probed by laser spray mass spectrometry. Rapid Communications in Mass Spectrometry, 2008, 22, 1430-1436.	0.7	14
114	Side-Chain Conformational Changes of Transcription Factor PhoB upon DNA Binding: A Population-Shift Mechanism. Journal of the American Chemical Society, 2010, 132, 12653-12659.	6.6	14
115	Structural and biochemical analyses of the human PAD4 variant encoded by a functional haplotype gene. Acta Crystallographica Section D: Biological Crystallography, 2011, 67, 112-118.	2.5	14
116	The nature of the vibronic coupling in a metalloporphyrin and its Raman scattering. Journal of Molecular Spectroscopy, 1977, 68, 335-358.	0.4	13
117	Dynamics of DNA in Chromatin and DNA Binding Mode to Core Protein. Journal of Biochemistry, 1983, 93, 665-668.	0.9	13
118	Automatized Parameterization of the Densityâ€functional Tightâ€binding Method. II. Twoâ€center Integrals. Journal of the Chinese Chemical Society, 2016, 63, 57-68.	0.8	13
119	Three human RNA polymerases interact with TFIIH via a common RPB6 subunit. Nucleic Acids Research, 2022, 50, 1-16.	6.5	13
120	Proton Nuclear Magnetic Resonance Study of a Selectively Deuterated Mouse Monoclonal Antibody: Use of Two-Dimensional Homonuclear Hartmann-Hahn Spectroscopy1. Journal of Biochemistry, 1989, 106, 361-364.	0.9	12
121	Cytochromedaxial ligand of thebd-type terminal quinol oxidase fromEscherichia coli. FEBS Letters, 1993, 335, 13-17.	1.3	12
122	Crystallization and X-ray Studies of the DNA-binding Domain of OmpR Protein, a Positive Regulator Involved in Activation of Osmoregulatory Genes in Escherichia coli. Journal of Molecular Biology, 1994, 235, 780-782.	2.0	12
123	The Interaction Mode of the Acidic Region of the Cell Cycle Transcription Factor DP1 with TFIIH. Journal of Molecular Biology, 2016, 428, 4993-5006.	2.0	12
124	Spinâ€flip approach within timeâ€dependent density functional tightâ€binding method: Theory and applications. Journal of Computational Chemistry, 2020, 41, 1538-1548.	1.5	12
125	A vibronic coupling in a degenerate electronic state via a nuclear momentum and an antisymmetric Raman scattering tensor. Journal of Chemical Physics, 1977, 67, 1009.	1.2	11
126	A Spectroscopic Study of Hydrogen-bonds Involving the 2-Thiouracil Residue. Bulletin of the Chemical Society of Japan, 1980, 53, 1881-1887.	2.0	11

#	Article	IF	CITATIONS
127	Investigation of molecular size of transcription factor TFIIE in solution. Proteins: Structure, Function and Bioinformatics, 2005, 61, 633-641.	1.5	11
128	Long-term pulmonary complications of chemical weapons exposure in former poison gas factory workers. Inhalation Toxicology, 2016, 28, 343-348.	0.8	11
129	Nuclear magnetic resonance study on the interaction of aclacinomycin-A with a deoxyribo-hexanucleotide pentaphosphate d(CCTAGG)2 in aqueous solution Chemical and Pharmaceutical Bulletin, 1986, 34, 4494-4499.	0.6	10
130	Two metal-binding sites in a lead ribozyme bound to competitively by Pb2+ and Mg2+ . Induced structural changes as revealed by NMR. FEBS Journal, 1998, 255, 727-733.	0.2	10
131	NMR Dynamics Distinguish Between Hard and Soft Hydrophobic Cores in the DNA-binding Domain of PhoB and Demonstrate Different Roles of the Cores in Binding to DNA. Journal of Molecular Biology, 2007, 367, 1093-1117.	2.0	10
132	Mass Spectrometric Approach for Characterizing the Disordered Tail Regions of the Histone H2A/H2B Dimer. Analytical Chemistry, 2015, 87, 2220-2227.	3.2	10
133	Nucleosome organization and chromatin dynamics in telomeres. Biomolecular Concepts, 2015, 6, 67-75.	1.0	10
134	Recent advances in quantumâ€mechanical molecular dynamics simulations of proton transfer mechanism in various waterâ€based environments. Wiley Interdisciplinary Reviews: Computational Molecular Science, 2020, 10, e1419.	6.2	10
135	Hierarchical parallelization of divideâ€andâ€conquer density functional tightâ€binding molecular dynamics and metadynamics simulations. Journal of Computational Chemistry, 2020, 41, 1759-1772.	1.5	10
136	Structural and dynamical insights into the PH domain of p62 in human TFIIH. Nucleic Acids Research, 2021, 49, 2916-2930.	6.5	10
137	Difference of binding modes among three ligands to a receptor mSin3B corresponding to their inhibitory activities. Scientific Reports, 2021, 11, 6178.	1.6	10
138	Quantum-Mechanical Molecular Dynamics Simulations on Secondary Proton Transfer in Bacteriorhodopsin Using Realistic Models. Journal of Physical Chemistry B, 2021, 125, 10947-10963.	1.2	10
139	Raman and Solid State NMR Study on an Inclusion Compound of Aspartame with Cyclodextrin. Bulletin of the Chemical Society of Japan, 1986, 59, 93-96.	2.0	9
140	Dynamics of the Extended String-Like Interaction ofÂTFIIE with the p62 Subunit of TFIIH. Biophysical Journal, 2016, 111, 950-962.	0.2	9
141	Rate of photochemical protonation and electronic relaxation of excited 1, N6â€ethenoadenosine in its aqueous solution. Journal of Chemical Physics, 1981, 75, 3831-3837.	1.2	8
142	Histone tail network and modulation in a nucleosome. Current Opinion in Structural Biology, 2022, 75, 102436.	2.6	8
143	Raman spectrum of a closed-circular DNA. Biopolymers, 1985, 24, 1107-1111.	1.2	7
144	Quantum Chemical Calculations for up to One Hundred Million Atoms Using D <scp>cdftbmd</scp> Code on Supercomputer Fugaku. Chemistry Letters, 2021, 50, 1546-1550.	0.7	7

#	Article	IF	CITATIONS
145	2-Methylimidazole Does Not Bind to (Octaethylporphinato)iron(III) Chloride in the Presence of Methanol: A Resonance Raman Study. Journal of the American Chemical Society, 1994, 116, 4107-4108.	6.6	6
146	Structural characterization of human general transcription factor TFIIF in solution. Protein Science, 2008, 17, 389-400.	3.1	6
147	Infrared absorption spectrum of the simplest deuterated Criegee intermediate CD2OO. Journal of Chemical Physics, 2016, 145, 044305.	1.2	6
148	Infrared Spectra of Deoxyribonucleic Acids with Different Base Compositions in Their D2O Solutions. Bulletin of the Chemical Society of Japan, 1973, 46, 3891-3892.	2.0	5
149	RESONANCE RAMAN EFFECTS OF NUCLEOTIDES. Chemistry Letters, 1977, 6, 907-908.	0.7	5
150	A Raman spectroscopic analysis of the sequence-dependent structures of oligo-DNA duplexes: d(CGCG)2, d(GCGC)2, d(GGCC)2, and d(CCGG)2 in aqueous solution. Spectrochimica Acta Part A: Molecular Spectroscopy, 1986, 42, 1101-1106.	0.1	5
151	Quantum Chemical Estimation of Acetone Physisorption on Graphene Using Combined Basis Set and Size Extrapolation Schemes. Journal of Physical Chemistry C, 2017, 121, 8999-9010.	1.5	5
152	Mechanism of hERG inhibition by gating-modifier toxin, APETx1, deduced by functional characterization. BMC Molecular and Cell Biology, 2021, 22, 3.	1.0	5
153	Characteristic H3 N-tail dynamics in the nucleosome core particle, nucleosome, and chromatosome. IScience, 2022, 25, 103937.	1.9	5
154	Deuteration kinetics of N-methylacetamide by means of a stopped-flow multi-detector Raman spectrophotometry. Journal of Raman Spectroscopy, 1982, 12, 138-143.	1.2	4
155	A Possible Correlation between DNA Conformation and the Mode of Action of Restriction Enzymes1. Journal of Biochemistry, 1984, 96, 1807-1811.	0.9	4
156	Determination of the NMR solution structure of a specific DNA complex of the Myb DNA-binding domain. Journal of Biomolecular NMR, 1995, 6, 294-305.	1.6	4
157	A protein recycling system for nuclear magnetic resonance-based screening of drug candidates. Analytical Biochemistry, 2006, 353, 99-107.	1.1	4
158	Chargeâ€neutralization effect of the tail regions on the histone <scp>H</scp> 2 <scp>A</scp> / <scp>H</scp> 2 <scp>B</scp> dimer structure. Protein Science, 2015, 24, 1224-1231.	3.1	4
159	Is Oxygen Diffusion Faster in Bulk CeO2 or on a (111)-CeO2 Surface? A Theoretical Study. Chemistry Letters, 2021, 50, 568-571.	0.7	4
160	The Eaf3 chromodomain acts as a pH sensor for gene expression by altering its binding affinity for histone methylated-lysine residues. Bioscience Reports, 2020, 40, .	1.1	4
161	Crystallization of Arginine-, Formylmethionine-, Tyrosine-, and Glycine-Transfer RNAs from Escherichia coil. Journal of Biochemistry, 1978, 84, 369-375.	0.9	3
162	Anomalous temperature dependence of the phosphorus-31 nuclear magnetic resonance chemical shift in d(CCGG) and d(CCTAGG) at the junction of the pyrimidine stack followed by the purine stack Chemical and Pharmaceutical Bulletin, 1986, 34, 3987-3993.	0.6	3

#	Article	IF	CITATIONS
163	Structural Insights into the Asymmetric Effects of Zinc-Ligand Cysteine Mutations in the Novel Zinc Ribbon Domain of Human TFIIEα for Transcription. Journal of Biochemistry, 2005, 138, 443-449.	0.9	3
164	Development of density-functional tight-binding repulsive potentials for bulk zirconia using particle swarm optimization algorithm. AIP Conference Proceedings, 2017, , .	0.3	3
165	Structure of a DNA octamer, d(CCTTAAGG)2 obtained by restrained molecular dynamics based on Raman and NMR data. Journal of Molecular Structure, 1991, 242, 119-133.	1.8	2
166	A Raman Spectroscopic Study on Conformations of DNA Oligomers: A Dominant Effect of an AA:TT Sequence Over Those of AT:AT and TA:TA Sequences on Determining Conformations of DNA Duplexes. Nucleosides & Nucleotides, 1994, 13, 1467-1481.	0.5	2
167	Stochastic Search of Molecular Cluster Interaction Energy Surfaces with Coupled Cluster Quality Prediction. The Phenylacetylene Dimer. Journal of Chemical Theory and Computation, 2013, 9, 3848-3854.	2.3	2
168	Release of DCDFTBMD Program. Journal of Computer Chemistry Japan, 2018, 17, A21-A27.	0.0	2
169	Density-Functional Tight-Binding Parameters for Bulk Zirconium: A Case Study for Repulsive Potentials. Journal of Physical Chemistry A, 2021, 125, 2184-2196.	1.1	2
170	Divide-and-Conquer Density-Functional Tight-Binding Molecular Dynamics Study on the Formation of Carbamate Ions during CO2 Chemical Absorption in Aqueous Amine Solution. Bulletin of the Chemical Society of Japan, 2018, 91, 318-318.	2.0	1
171	Cover Image, Volume 10, Issue 1. Wiley Interdisciplinary Reviews: Computational Molecular Science, 2020, 10, e1459.	6.2	1
172	NMR Screening of mSin3B Binding Compounds for the Interaction Inhibition with a Neural Repressor, NRSF/REST. , 2017, , 1-22.		1
173	Laser Raman microscope: Application on biological samples Journal of the Spectroscopical Society of Japan, 1990, 39, 323-334.	0.0	0
174	Crystallization and preliminary X-ray diffraction studies on the DNA-binding domain of the transcriptional activator protein PhoB fromEscherichia coli. Acta Crystallographica Section D: Biological Crystallography, 2002, 58, 1862-1864.	2.5	0
175	Comparison of DNA-Binding Activities Between hTRF2 and hTRFl with hTRF2 Mutants. , 2008, , 743-751.		0
176	Analysis Of Side-chain Dynamics Of PhoB Dna Binding/transactivation Domain Using Molecular Dynamics Simulations. Biophysical Journal, 2009, 96, 299a.	0.2	0
177	Structural Characterization of the Histone Multimers in the Gas Phase using Ion Mobility Mass Spectrometry and Molecular Dynamics Simulation. Biophysical Journal, 2014, 106, 464a.	0.2	0
178	Dataset for the NMR structure of the intrinsically disordered acidic region of XPC bound to the PH domain of TFIIH p62. Data in Brief, 2016, 6, 571-577.	0.5	0
179	Determination of the Solution Structure of Isolated Histone H2A-H2B Heterodimer by using CS-Rosetta. Biophysical Journal, 2017, 112, 488a.	0.2	0
180	Structural Polymorphism of DNA and Its Recognizing-Proteins Seibutsu Butsuri, 1993, 33, 142-147.	0.0	0

#	Article	IF	CITATIONS
181	Scattering Phenomena and Their Applications to the Spectroscopy. III. Applications of Raman Scattering (II) Journal of the Spectroscopical Society of Japan, 1995, 44, 163-168.	0.0	0
182	NMR Screening of mSin3B Binding Compounds for the Interaction Inhibition with a Neural Repressor, NRSF/REST. , 2018, , 705-726.		0
183	Surface Reaction Simulation based on Divide-and-Conquer Type Density Functional Tight-Binding Molecular Dynamics (DC-DFTB-MD) MethodÂ: Case for Proton Diffusion on Pt(111) Surface. Vacuum and Surface Science, 2019, 62, 486-491.	0.0	Ο
184	DIFFERENCE RAMAN SPECTROSCOPY WITH A STOPPED-FLOW DEVICE. , 1983, , 113-116.		0